Interfacial Melting of Ice in Contact with SiO_2

S. Engemann,[1] H. Reichert,[1] H. Dosch,[1,2] J. Bilgram,[3] V. Honkimäki,[4] and A. Snigirev[4]
[1]*Max-Planck-Institut für Metallforschung, Heisenbergstrasse 3, D-70569 Stuttgart, Germany*
[2]*Institut für Theoretische und Angewandte Physik, Universität Stuttgart, D-70569 Stuttgart, Germany*
[3]*Laboratorium für Festkörperphysik, ETH Zürich, CH-8093 Zürich, Switzerland*
[4]*European Synchrotron Radiation Facility, F-38043 Grenoble, France*
(Received 15 January 2004; published 17 May 2004)

The physical behavior of condensed matter can be drastically altered in the presence of interfaces. Using a high-energy x-ray transmission-reflection scheme, we have studied ice-SiO_2 model interfaces. We observed the formation of a quasiliquid layer below the bulk melting temperature and determined its thickness and density as a function of temperature. The quasiliquid layer has stronger correlations than water and a large density close to $\rho_{HDA} = 1.17$ g/cm^3 of high-density amorphous ice suggesting a structural relationship with the postulated high-density liquid phase of water.

DOI: 10.1103/PhysRevLett.92.205701 PACS numbers: 64.70.Dv, 61.10.Kw, 68.08.Bc

Water in its various forms is virtually omnipresent on Earth, and, without water, life would not be possible. Despite its importance and the amount of research devoted to the understanding of the structure and properties of water in ice [1], it still holds unsolved mysteries ranging from unusual response functions [2] to the melting behavior [3].

The melting transition of a solid is characterized by the loss of long-range translational order. Therefore, all Fourier components of the long-range order, i.e., the Bragg reflections, are affected as the relevant order parameters [4]. Only the average density as the zero order Fourier component is conserved with a slight but discontinuous change across the transition. The ice-water phase transition exhibits two particular interesting features linked to the average density, which are in some respects in theoretical conflict: One is pressure-induced melting which is mediated by the anomalous density increase upon melting from the low density of the Ih ice structure ($\rho_s = 0.92$ g/cm^3) to the high density of water ($\rho_l = 1.0$ g/cm^3 at 273 K). The Clausius-Clapeyron relation then leads to the well-known negative slope of the melting curve $T_m(p)$.

The other phenomenon is surface-induced melting, i.e., the appearance of a macroscopic quasiliquid layer at the surface of ice well below T_m. This effect also occurs in other materials [5,6] but is particularly pronounced in the case of ice. Typically 15 K below the bulk melting temperature, the surface of ice becomes unstable with respect to surface melting [7]. While surface melting of ice is well established experimentally, confirmed by many different techniques [7–10], it should not occur according to the "Hamaker criterion," which is based on a rather general expression for the interfacial energy gain or penalty upon the formation of a premelting quasiliquid layer [11]. The negative density gradient $\Delta\rho = (\rho_s - \rho_l)$ between the solid and liquid phase renders the Hamaker constant negative and the surface melting energetically unfavorable [12].

In the case of interfacial melting a new interface between the quasiliquid layer and the mineral occurs (see Fig. 1); therefore, the Hamaker argument no longer holds in its original form [13], and it is *a priori* not clear whether an interfacial quasiliquid layer emerges below the bulk melting point. While the occurrence of interfacial melting of ice itself has important environmental and technological consequences [3], there are no studies of the interfacial melting scenario with high spatial resolution reaching down to atomic length scales [14]. Since the average density exhibits anomalous behavior across the melting transition of ice, it is particularly interesting to directly probe the density and its profile across the interface by x-ray reflectivity techniques.

In order to investigate the effect of an interface on the melting of ice, we have prepared a model-type ice-mineral interface by contacting high-purity single crystal ice with amorphous SiO_2. This interface might serve as a model for ice-rock interfaces as they appear in nature. By x-ray reflectivity we investigated *in situ* the thermal behavior of this ice-SiO_2 interface during heating and cooling and found indeed clear-cut evidence for interfacial melting. Most intriguingly, we also discovered that the emerging interfacial layer exhibits a strongly enhanced density compared to bulk water.

For a direct probe of the existence of any interfacial quasiliquid layer, we use a new x-ray diffraction scheme [15], exploiting highly brilliant high-energy x rays provided at third generation synchrotron radiation sources

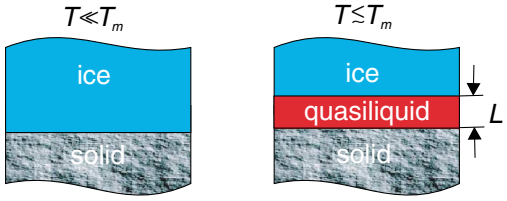

FIG. 1 (color). Scenario for interface melting of ice at an inhomogeneous interface upon approaching the melting point T_m.

and compound refractive x-ray lenses [16]. It allows one to produce penetrating high-energy x-ray beams with μm cross section and high collimation which are the ideal *in situ* probe of ice-solid interfaces. At the European Synchrotron Radiation Facility such an experimental setup has recently been installed at beam line ID15A (Fig. 2) [15]. A monochromatic high-energy x-ray beam ($E = 71.3$ keV, $\Delta E/E = 0.2\%$) from a synchrotron radiation source is focused by 232 Al parabolic refractive lenses (CRL) to a size of 5 μm (vertical) by 15 μm (horizontal) at the sample position. The x-ray beam penetrates the sample (24 mm long) at almost normal incidence from the side, thus illuminating only the ice-SiO_2 interface, and gets internally reflected at the ice-solid interface. The reflected beam has been monitored by a scintillation counter after vertical collimation to 46 μrad by a pair of adjustable slits. Typical reflected x-ray intensities as a function of perpendicular momentum transfer q are sketched on the right side of Fig. 2. A single interface gives rise to the smooth Fresnel curve (blue line), while an emerging quasiliquid layer with different density ρ_{qll} and thickness L produces interference fringes with an approximate period $2\pi/L$ in the reflectivity curve (red curve). Below the critical value q_c total reflection occurs. The measured reflectivity curve allows one to extract the microscopic density profile across the interfacial layer in a straightforward way [17].

In order to establish reproducible experimental conditions, the x-ray experiments were carried out on a well-defined ice-SiO_2 model system in a special sample cell which provides a well-controlled environment. A silicon block ($24 \times 24 \times 8$ mm^3) was polished to a roughness of 0.5 nm and cleaned with standard recipes (Piranha, RCA). At the final stage, the silicon block is covered by a thin layer of native amorphous SiO_2. The ice sample was thermally cut from a large single crystal with basal (00.1) orientation using clean metal wires. The ice surface was then polished with the smooth and clean silicon sample which was kept at 277 K. Moving the ice slowly against the silicon block allows one to flush impurities from the interface during the polishing process. Immediately after the polishing process the silicon block was slowly cooled, which led to recrystallization of the molten water layer at the interface. The sample was then sealed with a pure aluminum foil at ambient pressure and mounted between

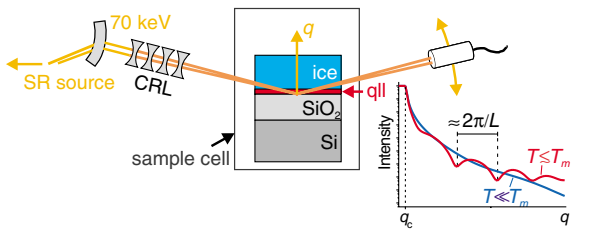

FIG. 2 (color). Sketch of the experimental setup (see the text).

two Peltier elements for cooling in the sample cell. Three calibrated Pt100 sensors were used for controlling and constantly monitoring the sample temperature. During the reflectivity measurements the background scattering and the integrated reflected intensity at each perpendicular momentum transfer q have been obtained from transverse momentum scans.

The temperature-dependent x-ray reflectivity profiles are summarized in Fig. 3(a). For low temperatures, they show the characteristic Fresnel curve modified by surface roughness at the ice-SiO_2 interface [see the corresponding density profile in the lower part of Fig. 3(b)]. Upon heating an additional x-ray intensity starts to emerge at high q values which gets gradually shifted to lower q values and finally develops to pronounced interference fringes. The effect is fully reversible and, thus, a direct evidence for the emergence of an equilibrium interfacial layer between ice and SiO_2 with a noticeably different density and rather well-defined interfaces [see the upper part of Fig. 3(b)].

From a detailed but rather straightforward analysis of the x-ray reflectivity profiles [full curves in Fig. 3(a)] the density profile [for a structural model, see Fig. 3(c) associated with $T = T_m - 1$ K] and its temperature dependence can be retrieved with subnanometer resolution providing direct insight into the thickness [$L(T)$] and density [$\rho_{\mathrm{qll}}(T)$] of the quasiliquid layer [Figs. 4(a) and 4(b)] as a function of distance to the solid surface. Three different approaches were used to obtain the density profile across the interface (kinetic and dynamic x-ray reflectivity calculations as well as a phase inversion algorithm [17]).

The quasiliquid layer starts to emerge at an onset temperature of $T_0 = T_m - 17$ K with an uncertainty of ± 3 K, and then its thickness increases smoothly as the temperature approaches the bulk melting temperature of ice [Fig. 4(a)], thereby following in a very good approximation a logarithmic growth law [straight line in Fig. 4(a)],

$$L(T) = a(0) \ln \frac{T_m - T_0}{T_m - T}, \tag{1}$$

which is expected from the theory of equilibrium wetting. The constant $a(0)$ corresponds here to the decay length of the nonordering (average) density as measured at the in-plane momentum transfer $q_{||} = 0$ [19]. From the slope in Fig. 4(a) we obtain $a(0) = (0.84 \pm 0.02)$ nm. This value can be compared with the bulk water correlation length with experimentally determined values ranging from $\xi_l = 0.45$ nm [20] to $\xi_l = 0.8$ nm [21] as measured in the small angle ($q \to 0$) x-ray scattering regime. This suggests that the observed nanosized premelting layer intercalated between ice and SiO_2 exhibits stronger local correlations than bulk water. This conclusion is corroborated by the measured average density $\rho_{\mathrm{qll}}(T)$ [Fig. 4(b)]

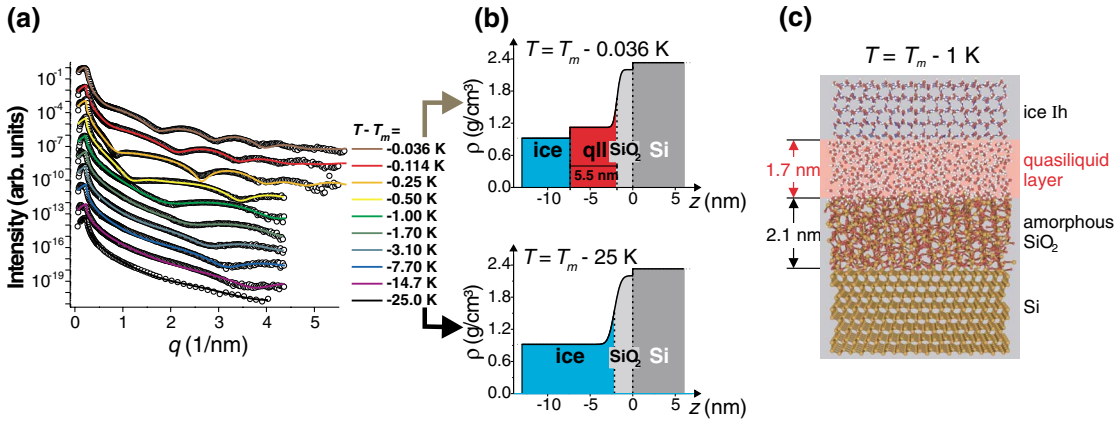

FIG. 3 (color). (a) Reflectivity curves of the ice-SiO_2 interface in the vicinity of the ice melting point. Solid lines are fits to the data using the (dynamical) Parratt formalism [18]. (b) $\rho(z)$ across the interface well below the onset temperature for interfacial melting ($T = T_m - 25$ K) and close to the melting point ($T = T_m - 0.036$ K). (c) Real space model of the ice-SiO_2 interface associated with $T = T_m - 1$ K. The densities used in this representation correspond to the values deduced from the measurement.

which reveals an intriguing phenomenon: Within the entire temperature range covered by our experiment, the observed average density of the interfacial quasiliquid layer is much higher than $\rho_l = 1.0$ g/cm^3 (bulk water), and close to 256 K where the quasiliquid layer starts to form, the density is as large as $\rho_{\mathrm{qll}} = 1.2$ g/cm^3. The data also show within the experimental error that the average density $\rho_{\mathrm{qll}}(T)$ tends to decrease to the asymptotic value $\rho_l = 1.0$ g/cm^3 for $(T - T_m) \to 0$ or, equivalently, for $L \to \infty$ [straight line in Fig. 4(b)]. We emphasize here that the strongly enhanced density of the premelting layer as deduced from the x-ray evidence is a very robust experimental fact. By our analysis we have model-independently verified that only a strongly enhanced density at the interface can account for the observed x-ray reflectivity profiles.

Figure 5 displays the low-pressure part of the water phase diagram, where H_2O can exist in several crystalline and amorphous forms, such as high-density amorphous (HDA) and low-density amorphous (LDA) ice. In current water theories [2,23,24], these are the vitreous counterparts of two different forms of liquid water—a low-density liquid phase (LDL) and a high-density liquid phase (HDL) (also shown in Fig. 5). Most striking, the measured density of the premelting layer is very close to the ambient pressure density of HDA ice, $\rho_{\mathrm{HDA}} = 1.17$ g/cm^3, pointing to a close structural relationship. However, since the observed interfacial premelting is an equilibrium phenomenon, one must assume that the observed quasiliquid layer is not governed by the vitreous HDA phase but rather by (equilibrium) fluctuations of the hypothetical liquid HDL phase. Then, as the thickness of the premelting layer grows, fluctuations of the LDL phase would progressively become possible and give rise to the observed decrease of the average density. This scenario, suggested by the experimental evidence, raises the question why the particular nanosized geometry provided by the interface-premelting scenario favors the appearance of fluctuations into the HDL phase and to which extent the structure and/or chemistry of the ice-SiO_2 interface is important. If these questions are addressed by theoretical arguments, the experimental conditions (geometry and chemistry) could be tailored to stabilize and then study one particular water fluctuation.

The observed interfacial melting has important ramifications for environmental phenomena [3], as permafrost and the motion of glaciers. Since these effects depend on the mechanical properties of the interfacial layer, the

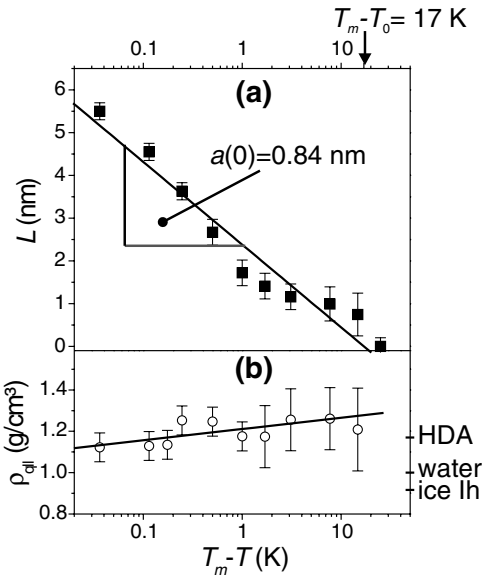

FIG. 4. (a) Temperature dependence of the thickness L of the quasiliquid layer. The straight line is a fit to a logarithmic growth law. (b) Temperature dependence of the average density ρ_{qll} in the quasiliquid layer. The fitted (straight) line indicates the trend for a decreasing average density with growing layer thickness.

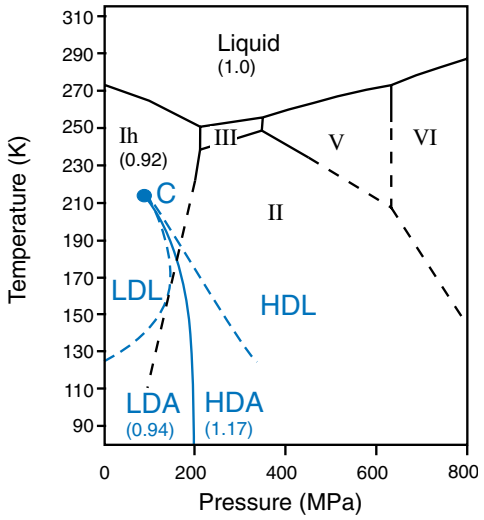

FIG. 5 (color). Phase diagram of water at moderate pressures compiled from Refs. [1,22]. The dashed blue lines terminating in a tentative critical point C separate low density and high density water from low density and high density amorphous ice. The numbers in parentheses denote the densities (at atmospheric pressure).

observation of a high-density phase of water instead of bulk water at the interface is particularly interesting. The environmental impact of interfacial melting is also determined by the solubility of impurities such as Na, Cl, or Br [25] in the premelting quasiliquid. For bulk systems it is known that most impurities have a small solubility in ice and a large solubility in water. In the case of large solubility in the high-density premelting quasiliquid, interfacial melting might spark a self-amplifying process, where enrichment of impurities in the quasiliquid layer leads to a true reduction of the melting temperature.

In conclusion, we have shown that ice in contact with a SiO_2 model interface exhibits interfacial melting. It features the characteristics of a wetting transition in the temperature range covered by the experiment. The strong confinement of the quasiliquid between ice and SiO_2 leads to an equilibrium high-density structure. Future experiments determining the liquid structure factor parallel to the interface will clarify the relation with the postulated high-density phases (liquid or amorphous) of water.

This work has been funded by the Deutsche Forschungsgemeinschaft in the priority program on "wetting and structure formation at interfaces" and by the Swiss National Science Foundation (J. B.).

[1] V. F. Petrenko and R.W. Whitworth, *Physics of Ice* (Oxford University Press, Oxford, 1999).
[2] P. G. Debenedetti and H. E. Stanley, Phys. Today **56**, No. 6, 40 (2003).
[3] J. G. Dash, H.-Y. Fu, and J. S. Wettlaufer, Rep. Prog. Phys. **58**, 115 (1995).
[4] R. Lipowsky, U. Breuer, K. C. Prince, and H. P. Bonzel, Phys. Rev. Lett. **62**, 913 (1989); H. Löwen and T. Beier, Phys. Rev. B **41**, 4435 (1990).
[5] J. F. van der Veen, B. Pluis, and D. van der Gon, in *Chemistry and Physics of Solid Surfaces VII*, edited by R. Vanselow and R. F. Howe (Springer, Berlin, 1988), p. 455.
[6] J. G. Dash, Contemp. Phys. **30**, 89 (1989).
[7] A. Lied, H. Dosch, and J. H. Bilgram, Phys. Rev. Lett. **72**, 3554 (1994).
[8] D. Nason and N. H. Fletcher, J. Chem. Phys. **62**, 4444 (1975).
[9] M. Elbaum, S. G. Lipson, and J. G. Dash, J. Cryst. Growth **129**, 491 (1993).
[10] Xing Wei, P. B. Miranda, and Y. R. Shen, Phys. Rev. Lett. **86**, 1554 (2001).
[11] R. Lipowsky, Ferroelectrics **73**, 69 (1987).
[12] M. Elbaum and M. Schick, Phys. Rev. Lett. **66**, 1713 (1991).
[13] L. A. Wilen, J. S. Wettlaufer, M. Elbaum, and M. Schick, Phys. Rev. B **52**, 12 426 (1995).
[14] M. Maruyama, M. Bienfait, J. G. Dash, and G. Coddens, J. Cryst. Growth **118**, 33 (1992); D. Beaglehole and P. Wilson, J. Phys. Chem. **98**, 8096 (1994); B. Pittenger *et al.*, Phys. Rev. B **63**, 134102 (2001).
[15] H. Reichert *et al.*, Physica (Amsterdam) **336B**, 46 (2003).
[16] B. Lengeler *et al.*, Appl. Phys. Lett. **74**, 3924 (1999).
[17] M. Tolan, *X-Ray Scattering From Soft-Matter Thin Films* (Springer, Berlin, 1999).
[18] L. G. Parratt, Phys. Rev. **95**, 359 (1954).
[19] R. Lipowsky, in *Magnetic Properties of Low-Dimensional Systems II*, edited by by L. M. Falicov, F. Mejia-Lira, and J. L. Moran-Lopez (Springer, Berlin, Heidelberg, 1990), p. 158.
[20] Y. L. Xie *et al.*, Phys. Rev. Lett. **71**, 2050 (1993).
[21] L. Bosio, J. Teixeira, and H. E. Stanley, Phys. Rev. Lett. **46**, 597 (1981).
[22] O. Mishima and H. E. Stanley, Nature (London) **396**, 329 (1998).
[23] P. H. Poole, F. Sciortino, U. Essmann, and H. E. Stanley, Nature (London) **360**, 324 (1992).
[24] S. Sastry, P. G. Debenedetti, F. Sciortino, and H. E. Stanley, Phys. Rev. E **53**, 6144 (1996).
[25] J. S. Wettlaufer, Phys. Rev. Lett. **82**, 2516 (1999).